Journal of Cerebral Blood Flow & Metabolism (2014) 34, 1453–1462

www.jcbfm.com

ORIGINAL ARTICLE

The vascular steal phenomenon is an incomplete contributor to negative cerebrovascular reactivity in patients with symptomatic intracranial stenosis

Daniel F Arteaga[1], Megan K Strother[1], Carlos C Faraco[1], Lori C Jordan[2], Travis R Ladner[1], Lindsey M Dethrage[1], Robert J Singer[3], J Mocco[4], Paul F Clemmons[5], Michael J Ayad[6] and Manus J Donahue[1,2,7,8]

'Vascular steal' has been proposed as a compensatory mechanism in hemodynamically compromised ischemic parenchyma. Here, independent measures of cerebral blood flow (CBF) and blood oxygenation level-dependent (BOLD) magnetic resonance imaging (MRI) responses to a vascular stimulus in patients with ischemic cerebrovascular disease are recorded. Symptomatic intracranial stenosis patients ($n = 40$) underwent a multimodal 3.0T MRI protocol including structural (T_1-weighted and T_2-weighted fluid-attenuated inversion recovery) and hemodynamic (BOLD and CBF-weighted arterial spin labeling) functional MRI during room air and hypercarbic gas administration. CBF changes in regions demonstrating negative BOLD reactivity were recorded, as well as clinical correlates including symptomatic hemisphere by infarct and lateralizing symptoms. Fifteen out of forty participants exhibited negative BOLD reactivity. Of these, a positive relationship was found between BOLD and CBF reactivity in unaffected (stenosis degree $< 50\%$) cortex. In negative BOLD cerebrovascular reactivity regions, three patients exhibited significant ($P < 0.01$) reductions in CBF consistent with vascular steal; six exhibited increases in CBF; and the remaining exhibited no statistical change in CBF. Secondary findings were that negative BOLD reactivity correlated with symptomatic hemisphere by lateralizing clinical symptoms and prior infarcts(s). These data support the conclusion that negative hypercarbia-induced BOLD responses, frequently assigned to vascular steal, are heterogeneous in origin with possible contributions from autoregulation and/or metabolism.

Journal of Cerebral Blood Flow & Metabolism (2014) **34,** 1453–1462; doi:10.1038/jcbfm.2014.106; published online 11 June 2014

Keywords: BOLD; cerebral blood flow; hemodynamics; MRI; stenosis; stroke

INTRODUCTION

Intracranial (IC) arterial stenosis is an important risk factor for ischemic stroke, with 2-year stroke rates approaching 20% in those with symptomatic disease.[1] While preventive procedures such as revascularization angioplasty and endovascular stenting are available, identifying patients that would benefit most from these interventions remains problematic. The need for risk stratification was recently highlighted in a multicenter clinical trial, which revealed that angioplasty and endovascular stenting increased the probability of stroke compared with aggressive medical management alone.[2]

More sensitive radiologic screening procedures that can be used safely to track hemodynamic progression and therapy response are likely required to improve management decisions. Digital subtraction angiography is the gold standard for measuring arterial luminal stenosis. However, digital subtraction angiography is invasive and insensitive to tissue-level hemodynamics such as cerebral blood flow (CBF; mL/100 g/minute) and volume (CBV; mL blood/mL parenchyma). Positron emission tomography and single-photon emission computed tomography can measure these parameters, but are currently suboptimal owing to limited availability of these technologies and the required tracers in non-specialized centers.

Non-invasive magnetic resonance imaging (MRI) has emerged as a promising tool that can provide complementary information about structural and hemodynamic changes. Magnetic resonance imaging protocols that exploit T_2 or T_2*-weighted blood oxygenation level-dependent (BOLD) contrast are capable of measuring parenchymal cerebrovascular reactivity (CVR) in response to vasodilatory stimuli, and this approach is being used with increasing frequency in cerebrovascular disease, dementia, and tumor applications.[3–5] However, fundamental gaps remain in our knowledge regarding the physiologic underpinnings of the BOLD contrast mechanism, and importantly how BOLD contrast in patients with vascular disease correlates with prognosis. As such, careful measurements of BOLD contrast in a clinical setting, together with corroborating data from separate modalities, is required before such imaging can be incorporated routinely into the radiologic infrastructure as a diagnostic tool.

In healthy tissue, positive BOLD signal arises from increases in blood oxygenation as a result of larger increases in CBF relative to

[1]Department of Radiology, Vanderbilt University School of Medicine, Nashville, Tennessee, USA; [2]Department of Neurology, Vanderbilt University School of Medicine, Nashville, Tennessee, USA; [3]Department of Neurosurgery, Geisel School of Medicine, Dartmouth College, Lebanon, New Hampshire, USA; [4]Department of Neurological Surgery, Vanderbilt University School of Medicine, Nashville, Tennessee, USA; [5]Department of Radiology Nursing, Vanderbilt University School of Medicine, Nashville, Tennessee, USA; [6]Department of Neurological Surgery, New York Methodist Hospital, Brooklyn, New York, USA; [7]Department of Psychiatry, Vanderbilt University School of Medicine, Nashville, Tennessee, USA and [8]Department of Physics and Astronomy, Vanderbilt University, Nashville, Tennessee, USA. Correspondence: Dr MJ Donahue, Vanderbilt University Institute of Imaging Science, 1161 21st Avenue S, MCN, AAA-3115, Nashville, TN 37232–2310, USA.
E-mail: mj.donahue@vanderbilt.edu
This work was supported by the National Institutes of Health (5R01NS078828-02).
Received 31 January 2014; revised 1 May 2014; accepted 22 May 2014; published online 11 June 2014

the cerebral metabolic rate of oxygen consumption ($CMRO_2$). Hypercarbic stimuli, which are frequently used in BOLD CVR studies, have been reported to be primarily isometabolic in healthy tissue for short stimulus durations ($\leqslant$3 minutes).[6,7] As such, BOLD signal increases in healthy tissue in response to hypercarbia derive from an increase in CBF, which increases the fraction of diamagnetic oxyhemoglobin relative to paramagnetic deoxyhemoglobin, in capillaries and veins. Of note, such positive BOLD responses will be attenuated through T2(*) attenuation due to small increases in capillary and venous CBV. Given these characteristics, BOLD imaging in response to hypercarbic gas stimulation has been utilized as a surrogate marker of vascular compliance or CVR. Over a range of healthy flow-volume coupling indices, smaller increases in CBF will lead to smaller BOLD responses, hypothesized to be indicative of vasculature operating at or near reserve capacity.

Negative hypercarbia-induced BOLD effects have also been reported in patients with cerebrovascular disease, and these negative effects are commonly attributed to 'vascular intracerebral steal' phenomena whereby blood is re-routed from ischemic parenchyma to healthy parenchyma.[8,9] As the primary origin of hypercarbia-induced BOLD responses in healthy tissue is from CBF and CBV (e.g., vascular changes), these findings provide support, but do not confirm, the presence of vascular steal phenomena. Such negative BOLD effects have been shown to correlate inversely with cortical thickness and directly with IC vascular disease severity.[10]

The mechanism underlying negative BOLD responses, however, is controversial. Occlusion models in animals have demonstrated that hypercarbia does not change CBF in ischemic brain[11,12] and in subacute human stroke patients, it has been demonstrated that CBF response to hypercarbia is heterogeneous.[13] Understanding this phenomenon is fundamental to using BOLD contrast for routine radiologic imaging and for understanding the physiologic constructs of impairment.

In addition to vascular steal, two additional mechanisms may contribute to negative BOLD CVR: (i) cerebrovascular autoregulation and/or (ii) $CMRO_2$ upregulation. More specifically, changes in cerebral perfusion pressure may have little effect on CBF over a wide range due to cerebral autoregulation. Increases in arterial pressure produce vasoconstriction of pial arterioles, and decreases produce vasodilation, thus altering resistance and maintaining a CBF within a viable range.[14] Large increases in CBV relative to CBF could lead to negative BOLD effects, especially if the CBV changes occur in veins or arteries with low oxygen saturation fractions (e.g., hypoxic patients). Alternatively, an increase in the supply of oxygen may lead to an increase in $CMRO_2$ in mild-to-moderately ischemic tissue, which would lead to an increase in deoxyhemoglobin in capillaries and veins when CBF increases minimally, and this could contribute to a reduction in BOLD CVR. Representative scenarios by which negative BOLD CVR could be explained are shown in Figure 1. These scenarios have been simulated using standard equations from popular BOLD contrast models.[15,16]

To better understand the origins of negative BOLD CVR, we measure the CBF response in regions of negative BOLD reactivity in patients with symptomatic ischemic cerebrovascular disease, and contrast reactivity values with standard clinical measures of vascular stenosis and lateralizing disease severity.

MATERIALS AND METHODS

Patient Anonymity, Informed Consent, and Ethics

Anonymity of all volunteers was assured by removing the volunteers' names from data and figures. This study includes experiments on human subjects; procedures were followed in accordance with the ethical standards of the Vanderbilt University Institutional Review Board (IRB Study #110468), the Vanderbilt University Human Research Protection Program, as well as with the Helsinki Declaration of 1975 (and as revised in 1983). Informed written consent was obtained from all volunteers and all components of this study were in compliance with the Health Insurance Portability and Accountability Act (HIPAA). No animal studies were conducted as part of this work.

Participant Demographics

Patients ($n = 40$; age $= 54.5 \pm 17.7$ years; 17M/23F) presenting with angiographically confirmed IC stenosis and/or symptoms consistent with IC stenosis (Supplementary Table 1A and 1B) between 1 August 2012 and 1 August 2013 provided informed written consent in accordance with the local IRB and HIPAA guidelines. Participants with both atherosclerotic and non-atherosclerotic (i.e., moyamoya) disease were included. Owing to the known differing etiology of atherosclerotic and non-atherosclerotic IC stenosis, these groups were evaluated independently to understand whether different types of IC stenosis yield different negative BOLD CVR trends.

Lateralizing Signs

In patients, lateralizing signs on neurologic examination corresponding to both hemispheres were retrospectively assessed by review of the electronic medical record. Symptomatic hemispheres were defined as those with either a history of recurrent transient ischemic attacks or persisting neurologic deficits in the motor, sensory, or language domains. Psychological symptoms, personality deficits, deficits in concentration and memory, and headache were not considered for this analysis.

Magnetic Resonance Imaging

All participants were scanned at 3.0T (Philips Medical Systems; Best, The Netherlands). Standard T_1-weighted (three-dimensional turbo gradient echo; TR/TE = 8.9/4.6 ms; spatial resolution = 1 × 1 × 1 mm), T_2-weighted fluid-attenuated inversion recovery (turbo spin echo; TR/TE = 11,000/120 ms; spatial resolution = 1.9 × 1.9 × 5 mm), and three-dimensional time-of-flight magnetic resonance angiography imaging (three-dimensional gradient echo; TR/TE = 13.8/1.8 ms; spatial resolution = 1.3 × 1.3 × 1 mm) sequences were performed in addition to functional acquisitions with whole-brain BOLD (single-shot gradient echo-planar imaging; TR/TE = 2,000–4,000/35 ms; spatial resolution = 3 × 3 × 7 mm) and pseudocontinuous arterial spin labeling (pCASL; single-shot gradient echo-planar imaging; TR/TE = 4,000/17 ms; spatial resolution = 3 × 3 × 7 mm). The spatial resolution of BOLD was matched to that of ASL, and as such was coarser than what is normally obtained in other BOLD studies (e.g., typical slice thickness 3–5 mm); this choice was used to reduce the possibility of partial volume effects differing between scans (see Discussion). The ASL scan was always performed after the BOLD scan. In some patients ($n = 23$), a BOLD protocol with TR = 4,000 ms was used, whereas in the remainder ($n = 18$) TR = 2,000 ms was used. This discrepancy is not expected to influence the findings of this study as the stimulus duration was long (>3 min) relative to the temporal resolution. The pCASL sequence employed a 1.6 seconds labeling pulse train consisting of 0.5 ms Hanning-windowed pulses, followed by a post-labeling delay of 1.525 seconds. Pseudocontinuous arterial spin labeling parameters were based on multi-delay optimization work by us[17] and others[18,19] and pCASL specifically was chosen (i) owing to its higher signal-to-noise ratio relative to pulsed ASL approaches[20] and (ii) to increase the time from beginning of labeling to imaging to more than 3 seconds, which increases feasibility for measuring CBF in the regions of delayed bolus arrival time (BAT), such as in white matter or ischemic tissue.[18] Concerns related to changes in BAT with hypercarbic gas stimulation and partial volume effects have been considered by us and others in the literature and are summarized in the context of this study in the Discussion. A separate equilibrium magnetization (M_0) image was acquired with identical spatial resolution as the pCASL scan but with TR = 20 seconds and all spin labeling pulses removed. Delivery of medical grade room air (three blocks with 3 minutes duration each; ~21% O_2/78% N_2; <1% CO_2) was alternated with a hypercarbic gas mixture (two blocks of 3 minutes each; 5% CO_2/95% O_2) during the functional magnetic resonance imaging acquisitions. Hypercarbic hyperoxia (e.g., carbogen) was used as the vasodilatory stimulus owing to its ability to increase the fraction of inspired O_2 and oxygen delivery to tissue,[21] which was required as a conservative safety measure in our clinic owing to the possible side effects from a more simple hypercarbic normoxic (e.g., 5% CO_2/21% O_2/74% N_2) gas mixture. BOLD and pCASL contrasts were interpreted within the physiologic context of this more complex gas challenge (see Discussion). Gas delivery was achieved using a non-rebreathing

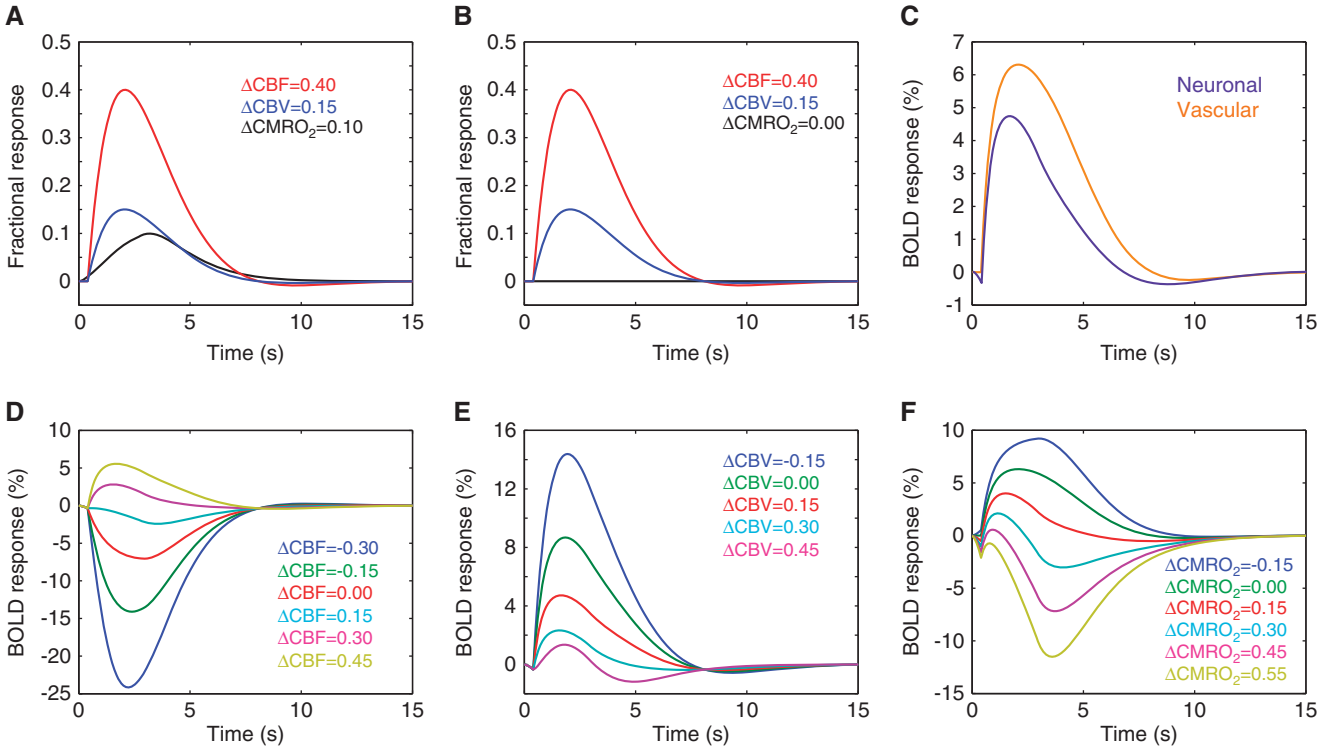

Figure 1. Different physiologic responses that could contribute to negative blood oxygenation level-dependent (BOLD) responses. Simulations are based on previously published BOLD contrast models and hemodynamic response functions and are simulated for a pure gray matter voxel. Healthy (**A**) neuronal and (**B**) isometabolic ($CMRO_2$) vascular reactivity elicit (**C**) different BOLD responses. The magnitude of the BOLD response depends on the balance of these changes (approximate responses at 3.0T shown), and it is not necessarily expected that cerebral blood flow (CBF) and volume (CBV) increase by the same fractional amount in response to neuronal and vascular stimuli. Additional physiologic scenarios are simulated below. Simulated BOLD responses to vascular stimulation for (**D**) varying CBF reactivity (ΔCBF) assuming fractional $\Delta CBV = 0.15$ and $\Delta CMRO_2 = 0$, (**E**) varying CBV reactivity (ΔCBV) assuming fractional $\Delta CBF = 0.40$ and $\Delta CMRO_2 = 0$, and (**F**) varying $CMRO_2$ reactivity ($\Delta CMRO_2$) for fractional $\Delta CBF = 0.40$ and $\Delta CBV = 0.15$. The range of changes is for exemplar purposes only and actual values will vary with disease and region considered. These curves demonstrate how (**D**) vascular steal (e.g., $\Delta CBF < 0$), autoregulation (e.g., $\Delta CBV \geq \Delta CBF$), and $CMRO_2$ upregulation (e.g., $\Delta CMRO_2 > 0$) could elicit negative BOLD responses.

facemask; end-tidal CO_2 ($EtCO_2$), heart rate, blood pressure, and arterial oxygen saturation were monitored throughout the exam (Medtronic, Minneapolis, MN, USA). Total protocol duration was ~40 minutes.

Data Analysis

A board-certified neuroradiologist (experience = 10 years) masked to clinical and imaging findings graded cerebrovascular stenosis and localized regions of infarct. For patients with moyamoya configuration, the modified Suzuki Score, which includes five stages of severity (see Supplementary Table 2), was used.[22,23] Intracranial stenosis was measured using previously published guidelines.[24] Stenosis degree and modified Suzuki Score were determined from vascular imaging acquired within 30 days of hemodynamic MRI as follows: (i) from clinical digital subtraction angiography if available; (ii) if no digital subtraction angiography, from CTA; (iii) if no CTA, from magnetic resonance angiography. Regions of interest were manually drawn by the neuroradiologist around areas of acute or subacute stroke and/or encephalomalacia on fluid-attenuated inversion recovery images. These regions were not considered as possible regions of negative CVR.

BOLD and pCASL analysis was performed using the FMRIB Software Library and MATLAB (MathWorks, Natick, MA, USA). Data from all subjects were corrected for motion and baseline drift.[25] Data were spatially smoothed (full-width half-maximum = 3 mm), and time points during the first 60 seconds of normocarbia and hypercarbia epochs were removed to allow for signal to reach steady state. Pseudocontinuous arterial spin labeling data were pairwise subtracted and normalized by M_0 to generate CBF-weighted maps, spatially smoothed to match the BOLD post-processing (full-width-half-maximum = 3 mm), and CBF was quantified upon application of the solution of the flow-modified Bloch equation assuming a blood–water T_1 reduction from 1.6 seconds to 1.4 seconds (effect of hyperoxia).[26,27] To enable comparison of negative regions between all subjects, BOLD and CBF-weighted maps were co-registered to a 4 mm isotropic Montreal Neurological Institute (MNI) T_1-weighted atlas.

Identification of patients with negative BOLD CVR was guided by *z*-statistic maps of the signal responses. *Z*-statistics were calculated using the FMRIB Expert Analysis Tool and the gas timing paradigm as a regressor, cluster size = 3 (corrected cluster $P < 0.05$). Additional criteria were applied to reduce possibilities that the negative CVR region was an artifact resulting from signal dropout, ventricular CSF, and/or delayed positive CVR. First, the floor of the anterior cranial fossa, where T_2*-weighted susceptibility-induced signal dropout occurred over the skull base, was excluded from analysis. Second, ventricles were masked from all images and negative BOLD CVR occurring in the ventricles was not considered. Third, regions of negative BOLD CVR that colocalized with prior infarcts, as identified on fluid-attenuated inversion recovery (see above), were excluded. Finally, time courses in negative CVR regions with a cluster-forming *P* value < 0.05 as determined from the FMRIB Software Library FMRIB Expert Analysis Tool analysis were evaluated visually, and it was required that the signal reduce below baseline during both stimulus blocks and also that the signal not have a delayed positive response (which could be misinterpreted as a negative response).

It is also important to ensure that the positive BOLD response is directly correlated with the positive CBF response in healthy tissue, as would be expected. To assess this, in all patients exhibiting negative BOLD effects, fractional reactivity maps (response relative to baseline denoted by $_0$) were calculated for BOLD signal ($\Delta S/S_0$) and CBF ($\Delta CBF/CBF_0$). These maps were co-registered to the MNI template and oriented such that the region with

the most significant stenosis (stenosis >50%) was on the radiologic right. A healthy tissue mask that consisted of cortical voxels within the Harvard/Oxford Cortical atlas for parietal, frontal, and occipital brain regions in the less-affected hemisphere was applied. The mask was modified to exclude voxels that partial volume predominately with dural sinuses, as these regions will contain BOLD signal that is largely specific to increases in oxyhemoglobin secondary to the hyperoxia administration. Parietal, frontal, and occipital regions were chosen, as these regions represent where negative BOLD CVR was consistently observed and therefore provide an approximate control when evaluated in the unaffected hemisphere.

Analysis and Statistical Considerations

The primary statistical goal of this study was to assess the directionality of the change in CBF-weighted pCASL signal between normocarbia and hypercarbia in the region of negative BOLD responses. To achieve this, CBF during normocarbia and hypercarbia was recorded in all participants with observed negative BOLD responses. The co-registered maps were used to ensure identical regions were analyzed. For analysis, a two-tailed Student's *t*-test (significance criteria $P<0.01$) was applied to test the mean difference

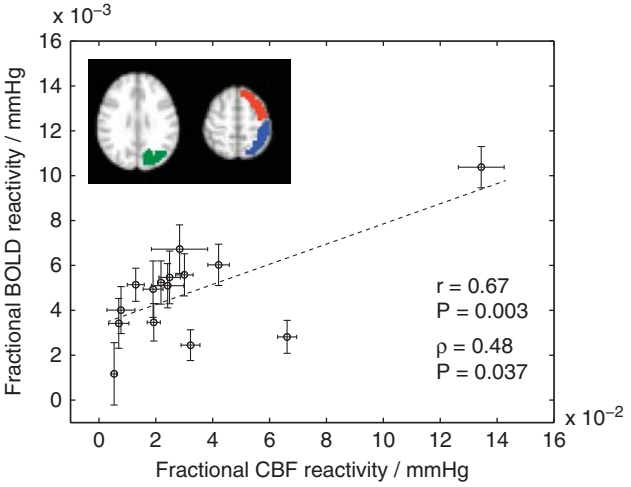

Figure 2. The relationship between blood oxygenation level-dependent (BOLD) and cerebral blood flow (CBF) response to hypercarbic hyperoxia (i.e., carbogen) in healthy appearing tissue (hemispheres with stenosis >50% oriented as radiologic right). Frontal (red), parietal (blue), and occipital (green) cortex regions used in the mask are shown (all voxels in all regions shown in scatter plot); regions of interest (ROIs) were based on the Harvard/Oxford cortical atlas but modified to exclude voxels that partial volume substantially with dural sinuses. This additional step was performed so that veins that are not expected to contribute to cerebrovascular reactivity but may be influenced substantially by hyperoxia are not considered. The scatter plot shows the fractional BOLD reactivity ($\Delta S/S_0$) and CBF reactivity ($\Delta CBF/CBF_0$) normalized by the change in end-tidal CO_2 (mm Hg). Error bars represent s.e. over the ROI, and therefore represent variability because of measurement inaccuracy, partial voluming, and physiology. The correlations between these two metrics were significant (Pearson's *R* and Spearman's ρ shown).

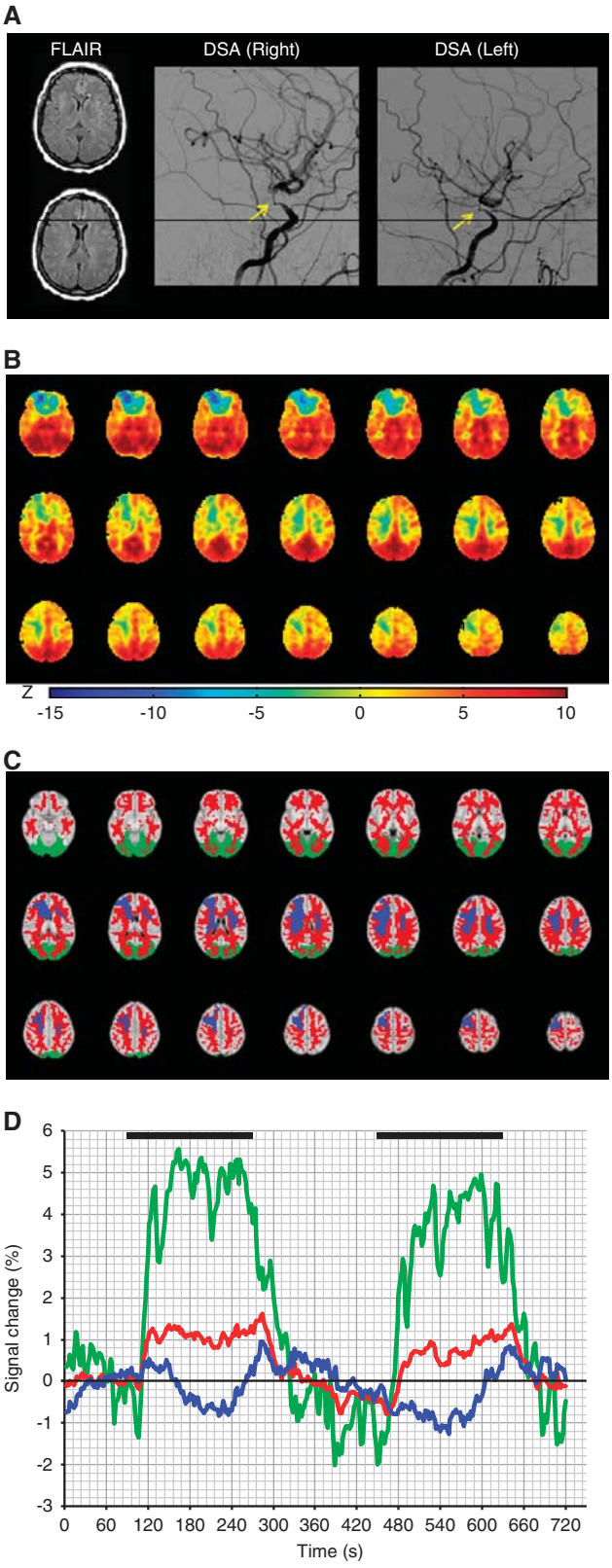

Figure 3. Time-course dynamics and cerebrovascular reactivity in patient 14, a 51–year-old female with bilateral moyamoya disease. (**A**) Axial fluid-attenuated inversion recovery (FLAIR) appears unremarkable at the level of negative blood oxygenation level-dependent (BOLD) reactivity. Lateral projections from common carotid artery injections from digital subtraction angiography (DSA) show severe right and left stenosis. (**B**) BOLD *z*-statistic maps show positive reactivity (*z*-statistic >0) throughout most of the cortex, but focal negative reactivity in the right frontal lobe (*z*-statistic <0). (**C**) Anatomic atlases for the white matter (red) and occipital lobe (green) were applied, together with the negative mask (blue) to calculate (**D**) the temporal dynamics of the BOLD response during normo- and hypercarbia. The focus of this work was to identify the directionality of blood flow responses in regions of such negative BOLD reactivity.

of CBF between the normocarbic and hypercarbic stimuli. To evaluate positive responses, for each subject the BOLD and CBF reactivity was calculated in the mask described above and was normalized by the change in $EtCO_2$ (mm Hg). To test the hypothesis that healthy BOLD CVR and CBF reactivity were positively correlated, one-sided Spearman's ρ and Pearson's R were calculated.

Descriptive statistics, including means, s.d., and ranges for continuous parameters were evaluated and investigations for outliers (defined as two s.d. beyond group mean) were performed.

RESULTS

Fifteen of 40 patients (age = 55.0 ± 16.4 years; 7M/8F) met the criteria for negative BOLD reactivity and were included in this analysis. Of these patients, four had moyamoya disease (age = 40.0 ± 11.7 years; 1M/3F) and 10 had non-moyamoya IC stenosis (age = 62.0 ± 14.1 years; 6M/4F); after careful review by the neuroradiologist, one patient (patient 12) had a left cavernous hemangioma without significant IC stenosis. Clinical presentation and history are shown in Supplementary Tables 1A, 1B, and 3 for all patients. End-tidal CO_2 increased by 6.2 ± 2.1 (mean ± s.d.) mm Hg, an acceptable range for increasing CVR. Figure 2 shows the relationship between BOLD and CBF reactivity in the healthy tissue mask. Responses in this region (mean ± s.d.) were 0.031 ± 0.012 and 0.23 ± 0.17 for BOLD and ASL, respectively.

Figure 3 shows representative images in a patient with moyamoya disease with negative BOLD reactivity. Figure 4 shows average BOLD and CBF data from all negative BOLD reactivity subjects. While clear asymmetry is apparent in the BOLD reactivity maps, the CBF maps are less asymmetric, suggesting that the BOLD reactivity maps have more complex contrast origins than can be described by CBF-weighted pCASL contrast alone.

Figure 5A shows negative BOLD CVR regions from all patients and Table 1 provides a summary of the measured BOLD and ASL values in patients exhibiting negative BOLD regions. All patients with unilateral IC steno occlusion exhibited negative BOLD CVR ipsilateral to the vascular stenosis. Twelve of 15 patients had negative CVR on the same side as their most severe vessel disease. Three patients (patients 9, 13, and 14) exhibited bilateral regions of negative CVR; BOLD and CBF data for these individuals were combined across hemispheres. Thirteen of 15 patients had prior cerebral infarcts (Supplementary Table 3). Although regions of encephalomalacia and subacute infarct were excluded before BOLD analysis, the negative BOLD effects still occurred ipsilateral to the infarct in 15 of 17 hemispheres. Thirteen symptomatic hemispheres were identified by lateralizing clinical symptoms, 10 of which were ipsilateral to the hemisphere with negative CVR.

The volume of negative BOLD regions varied across subjects (mean ± s.d.: voxels = 284 ± 532; volume = 22.0 ± 35.3 mL), and after correcting for statistical outliers weakly correlated inversely with reactivity in the same region ($R = -0.44$; one-tailed $P = 0.048$). No significant relationship was observed between the volume of steal and baseline CBF or the volume of the BOLD reactivity and CBF change with stimulus. In addition, there was no significant relationship between BOLD reactivity and $\Delta EtCO_2$ in either healthy cortex or the subject-specific negative masks, which was attributed to the $EtCO_2$ varying over a small range across subjects.

Figures 5B and 5C show differing hemodynamic responses to hypercarbia in two representative subjects. Within the negative

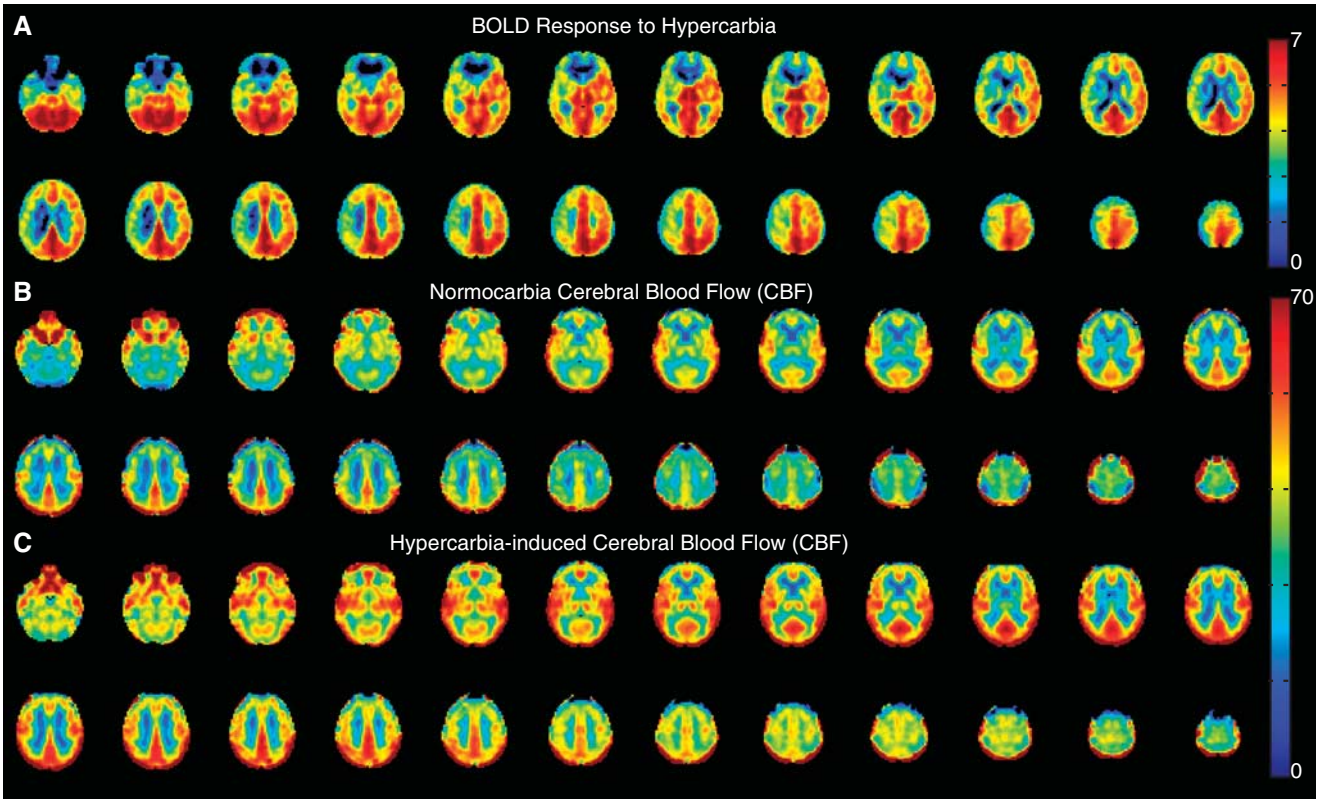

Figure 4. Mean blood oxygenation level-dependent (BOLD) and cerebral blood flow (CBF)-weighted arterial spin labeling (ASL) responses to hypercarbia in all participants ($n = 15$) exhibiting negative BOLD regions. Data have been co-registered to a 4 mm atlas and grouped such that radiologic right is the side of maximum stenosis or most severe moyamoya disease. Clear asymmetry is seen in the BOLD reactivity maps. While the axial CBF maps clearly increase with hypercarbia, asymmetry is less obvious, suggesting more complex mechanisms underlying the BOLD reactivity maps than can be explained by CBF-weighted ASL alone. The lower asymmetry in the CBF maps could also be because of a difference in bolus arrival time of healthy and ischemic tissue.

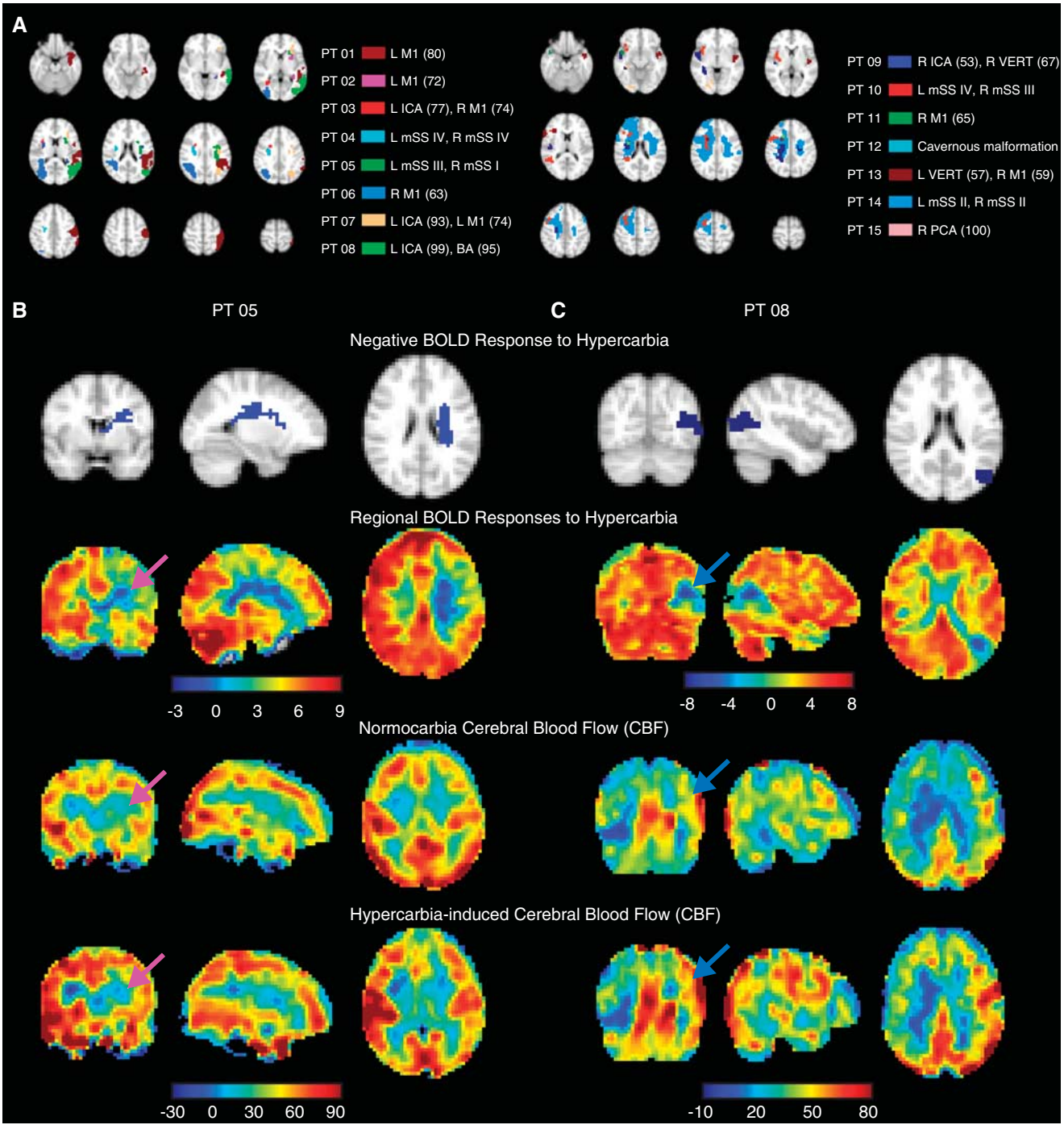

Figure 5. (**A**) Locations of negative blood oxygenation level-dependent (BOLD) reactivity in the 15 patients exhibiting negative BOLD effects. The 4 mm axial maps have been subdivided into two images for clarity. Example cases of a participant with (**B**; patient 5) and without (**C**; patient 8) apparent vascular intracerebral steal. Orthogonal slices of the negative BOLD reactivity regions (blue) are shown on top, followed by BOLD reactivity maps and baseline and hypercarbia-induced cerebral blood flow (CBF) maps below. The arrows identify the regions of negative BOLD reactivity. In these regions, clear and significant ($P<0.01$) decreases in CBF are found in patient 5, yet increases in CBF are observed in patient 8. These findings suggest that the origins of negative BOLD reactivity cannot be solely attributable to vascular intracerebral steal effects. Findings are compared with angiography in Figure 6. ICA, internal carotid artery; mSS, modified Suzuki score; PCA, posterior cerebral artery.

BOLD region, patient 5 exhibited significant ($P<0.01$) reductions in CBF and patient 8 exhibited significant increases ($P<0.01$) in CBF during hypercarbia administration. Structural imaging for both patients is shown in Figures 6A and 6B. When all patients exhibiting negative BOLD regions were considered (Table 1), three demonstrated significant reductions in CBF with hypercarbia in the negative BOLD region (patients 1, 5, and 10) consistent with vascular steal phenomena, yet six exhibited increases in CBF

Table 1. Imaging findings for patients with BOLD CVR

Patient	*Volume of negative BOLD CVR (mL)*	*Baseline CBF (mL/100 g/minute)*	*Activated CBF (mL/100 g/minute)*	*$\Delta EtCO_2$ (mm Hg)*	P *value (two-tailed)*	*Hemodynamic finding*
1	57.5	42.5 ± 1.2	9.3 ± 3.3	8.9	0.001	Steal
2	5.8	19.8 ± 2.1	16.9 ± 2.8	10.7	0.350	No change
3	2.8	3.3 ± 2.8	17.6 ± 2.6	5.3	0.001	Increase
4	4.3	3.2 ± 2.7	7.5 ± 2.5	6.9	0.012	No change
5	8.0	26.2 ± 2.1	18.9 ± 2.3	2.4	0.001	Steal
6	26.1	27.4 ± 0.9	36.5 ± 1.2	28.7[a]	0.001	Increase
7	7.8	21.0 ± 3.3	32.0 ± 2.7	6.6	0.005	Increase
8	23.4	50.8 ± 5.5	69.9 ± 6.8	6.6	0.001	Increase
9	18.9	47.5 ± 1.2	57.7 ± 1.7	4.8	0.001	Increase
10	19.5	19.3 ± 1.9	12.6 ± 2.3	4.4	0.002	Steal
11	1.9	23.0 ± 2.2	24.1 ± 3.9	8.1	0.714	No change
12	1.6	15.6 ± 7.2	16.0 ± 4.8	5.7	0.909	No change
13	9.2	32.6 ± 1.5	42.0 ± 2.3	5.6	0.001	Increase
14	138.2	18.8 ± 0.6	19.3 ± 0.5	5.7	0.032	No change
15	4.4	37.3 ± 1.9	41.3 ± 2.4	4.8	0.018	No change

BOLD, blood oxygenation level-dependent; CBF, cerebral blood flow; CVR, cerebrovascular reactivity; $\Delta EtCO_2$, change in end-tidal CO_2; MNI, Montreal Neurological Institute CBF values are shown as mean ± s.d. The volume of negative BOLD CVR is the volume of the identified region meeting negative BOLD criteria (see Materials and Methods) calculated in 4 mm MNI space. Statistical significance for hemodynamic findings accepted at $P < 0.01$. [a]Not included in mean calculation owing to equipment malfunction.

(patients 3, 6, 7, 8, 9, and 13) and the remaining six (patients 2, 4, 11, 12, 14, and 15) exhibited no statistical change in CBF with hypercarbia.

DISCUSSION

The primary finding of this study is that in patients with symptomatic IC stenoocclusive disease, regions of hypercarbic hyperoxic-induced negative BOLD reactivity cannot be exclusively explained by vascular steal phenomena. Rather, while a subgroup of cases do suggest steal phenomena, the majority of patients exhibited no or increased CBF response in these regions, suggesting that autoregulation or possible upregulation of $CMRO_2$ may contribute. Secondary findings are that negative BOLD reactivity correlates with symptomatic hemispheres both by imaging findings and lateralizing clinical symptoms. In addition, there is a weak inverse correlation ($P = 0.048$) between the volume of the negative CVR and the magnitude of the negative response.

Origins of Negative Blood Oxygenation Level-Dependent Cerebrovascular Reactivity in Patients

The magnitude of negative BOLD responses to hypercarbia have been reported to correlate indirectly with cortical thickness and directly with clinical disease severity, and have been hypothesized to represent a biomarker of infarction risk.[10] The physiologic origins of a negative BOLD response are known to occur in and around capillaries and draining veins from decreases in blood oxygenation, which could occur from reductions in CBF (vascular steal), increases in CBV (autoregulation), or upregulation of $CMRO_2$ (Figure 1). It should also be noted that while changes in venous CBV are generally smaller in magnitude than changes in arterial CBV, such changes influence BOLD substantially owing to the larger fraction of deoxyhemoglobin in veins. However, in patients with reduced arterial oxygen saturation fractions, arterial CBV changes may also begin to contribute measurably.

In prior acute stroke studies in humans, hypercapnia has not increased CBF in the ischemic brain. However, in subacute stages of stroke, the CBF response is more varied, with both increases and decreases in CBF reported.[13,28] Prior experimental and theoretical studies have demonstrated likely roles of elevated CBV secondary to reduced cerebral perfusion pressure.[29,30] Such autoregulation occurs actively through relaxation of smooth muscle surrounding arterioles rather than from bulk changes in venous CBV. Furthermore, some negative BOLD regions found here were observed in regions of white matter where CBV is low (0.01–0.02 mL blood/mL parenchyma), and these regions would require extremely large CBV changes to account for the magnitude of the observed BOLD signal reductions. An alternative option that warrants further investigation is that $CMRO_2$ may increase during the hypercarbic hyperoxia stimulus, as hypoxic tissue at baseline may metabolize the additional oxygen provided. This possibility is particularly intriguing, as it suggests that hyperoxia may provide a surrogate marker of impaired $CMRO_2$, which is a crucial physiologic parameter yet one that has been difficult to measure with MRI approaches.

Additional changes are known to occur from bulk relocalization of water in different compartments within a voxel (e.g., CSF and tissue),[31] and care was taken to avoid ventricles and infarcted regions in this study. It is possible that some negative BOLD CVR regions partly colocalize with cortical CSF (e.g., Patients 1 and 8); however, in the majority of patients it is unlikely that this contribution is dominant. An increase in CBV in these regions could relocate CSF across voxels; CSF has a higher water content, as well as a longer T_1 and T_2 relative to gray and white matter, and this could influence BOLD signal depending on the extent of water relocalization. This possibility has been investigated in the CBV literature,[32,33] as well as the presence of extravascular BOLD effects in CSF,[34] and may be present to varying extents in patients that contain negative BOLD signal near ventricles or regions of cortical CSF.

Hypercarbic Hyperoxia

Our study utilized a hypercarbic (5% CO_2) hyperoxic (95% O_2) stimulus, which has been employed previously in other studies and has been shown to correlate with disease severity in stenosis patients.[35] It is well known that hyperoxia will both increase BOLD signal in draining veins in a manner not related specifically to changes in hemodynamic or metabolic activity, and increase the partial pressure of arterial oxygen (PaO_2) and reduce the T_1 of blood water, complicating CBF quantification from ASL data. To ensure that healthy, positive BOLD reactivity was correlated with positive CBF reactivity to this stimulus, we recorded these values

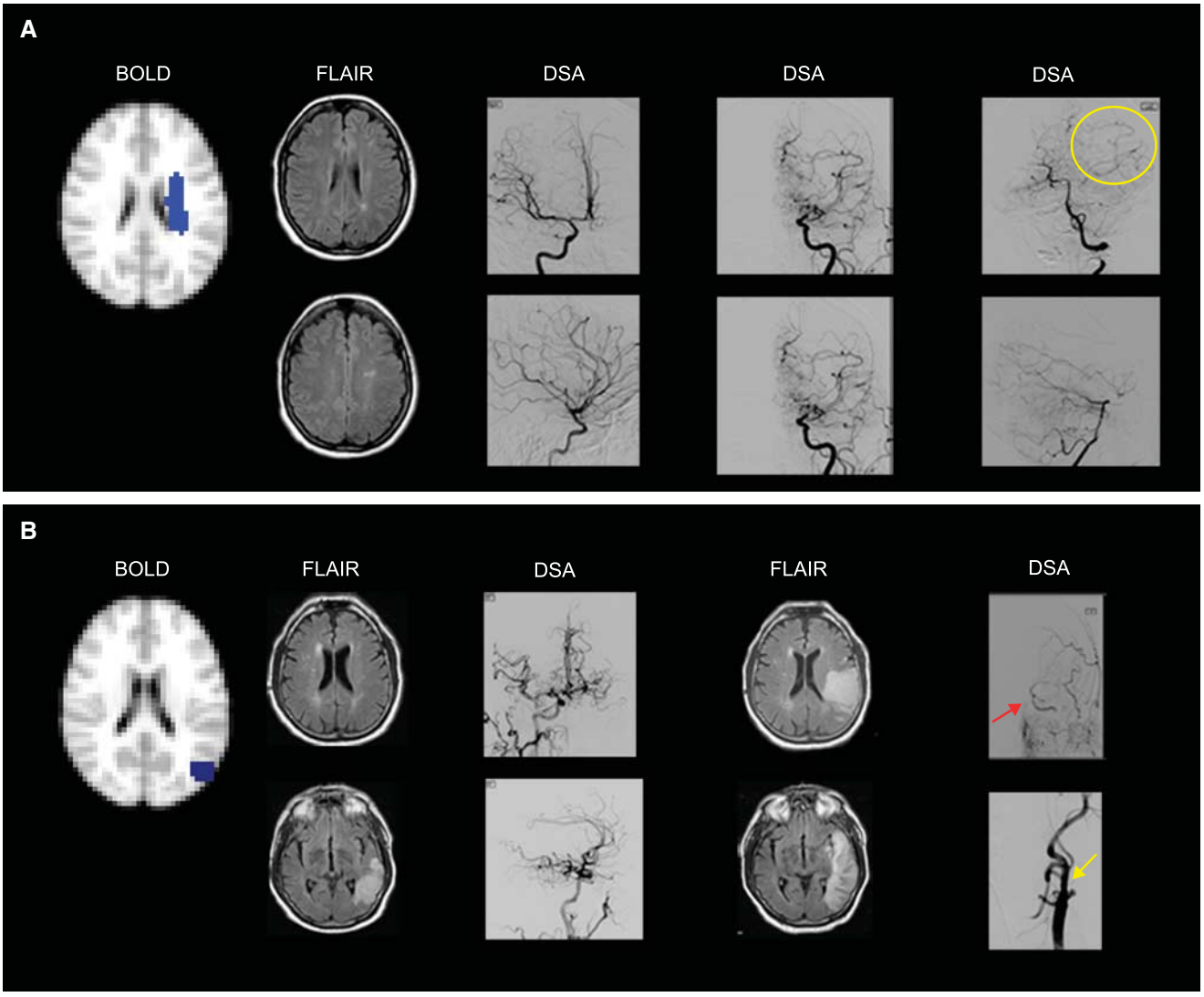

Figure 6. (**A**) Negative cerebrovascular reactivity (CVR) as a result of vascular steal is seen in the left centrum semiovale of a 25–year-old female with moyamoya disease. Fluid-attenuated inversion recovery (FLAIR) images show remote infarcts in the watershed distribution of the left hemisphere. Anterior–posterior (AP) and lateral projections from digital subtraction angiography (DSA) performed 1 week before hemodynamic magnetic resonance imaging (MRI) show (left DSA image) mild stenosis around the carotid bifurcation with slightly developed internal carotid artery (ICA) moyamoya (modified Suzuki score, mSS I) on the right after right ICA injection, (middle DSA image) occlusion of both the anterior cerebral artery and middle cerebral artery with well-developed ICA moyamoya (mSS III) on left external carotid artery (ECA) injection, and (right DSA image) extensive leptomeningeal collaterals from the posterior circulation to the anterior circulation upon left vertebral injection (yellow circle). (**B**) Negative CVR with increased cerebral blood flow in the left parietal cortex in a 72-year-old male with atherosclerotic intracranial disease. Fluid-attenuated inversion recovery images (left FLAIR image) at the time of hemodynamic MRI show a left posterior temporal–occipital infarct inferior to the region with negative reactivity (participant presented with acute aphasia 2 days before hemodynamic MRI). Anterior–posterior and lateral projection from DSA after right common carotid artery (CCA) injection shows (left DSA image) extensive cross-filling of the left cerebral hemisphere via the anterior communicating artery. Eight days later, FLAIR images (right FLAIR image) from a second MRI show the progression of the infarct to the region of negative CVR. The participant's aphasia had worsened with stroke extension that occurred when his blood pressure fell at a rehabilitation facility, 4 days after hemodynamic MRI. Anterior–posterior projections from left CCA injections show (right DSA image) collateral flow from the ECA to the intracranial ICA (red arrow) distal to the occluded cervical ICA stump (yellow arrow).

in healthy tissue (Figure 2) and found significant correlations using both Spearman and Pearson correlation tests. Care was taken to analyze data in tissue rather than draining veins, and indeed we found the relationship between BOLD and ASL responses to be much more variable in regions that partial volume significantly with the dural sinuses. Differences in regions considered may partly explain why these findings differ from other results that compared BOLD and CBF reactivity to hypercarbic hyperoxia.[27]

Our findings are also approximately consistent with physiology expectations; as the oxygen being extracted by the brain remains largely unchanged during vascular stimulation, extra oxygen carried in arterial plasma will substantially increase PaO_2 and some will bind Hb on the venous side. While this will contribute to the BOLD signal increase, the effect of hyperoxia on blood vasculature itself, in terms of decreasing CBV and CBF, have been shown to be small.[21] Therefore, complications arising from

carbogen administration are largely attributable to the effect of hyperoxia on the imaging signal (e.g., through increases in venous oxygen saturation and blood–water T_1 reduction) rather than from physiologic changes in vascular reactivity. It should thus be possible to partly control these effects using appropriate post-processing procedures, although more work is required to fully understand how to resolve these important limitations. As such, we strongly advise that hypercarbic hyperoxic and hypercarbic normoxic challenges should not be directly compared.

An alternative and certainly more straightforward challenge would be to administer hypercarbic normoxia (5% CO_2 with balance room air). The choice for our gas mixture was two-fold. First, many patients scanned in this study had severe neurovascular compromise, including recent strokes in some, which led to safety concerns regarding administering hypercarbic gas mixtures.[36] One of the long-term goals of this work is to incorporate gas challenges into routine radiologic protocols of subacute stroke patients, and it is unclear whether hypoxic or hypercarbic mixtures will elicit new ischemic events relative to hypercarbic hyperoxic mixtures that increase oxygen transport to tissue.[21] Safety has not yet been conclusively demonstrated in randomized clinical trials, and as such, many centers may resist hypercarbic normoxic gas administration in subacutely or even chronically ischemic patients. Second, the possibility of upregulation of $CMRO_2$ may not be expected in normoxia experiments, as there would be no obvious operative mechanism. Thus, while the hyperoxic component of the stimulus complicates interpretation, it may also reveal novel mechanisms of hemodynamic impairment that correlate more closely with infarction risk.

Experimental and Analysis Limitations

It is well known that in addition to CBF sensitivity, ASL contrast is dependent on the BAT, or the time for labeled blood water to reach the capillary exchange site.[37,38] Furthermore, while the ASL signal change in response to a stimulus is generally attributed to a change in CBF, it is also likely that the BAT changes. In separate work,[17] we have measured the BAT and CBF response using pCASL with multiple post-labeling delays in healthy volunteers (age $= 30 \pm 4$ years) for separate experiments in which (i) normocarbic normoxia (i.e., room air), hypercarbic normoxia (i.e., 5% CO_2/21% O_2/74% N_2), and hypercarbic hyperoxia (i.e., carbogen: 5% CO_2/95% O_2) gas was administered (12 L/minute). Regional reductions in BAT of 4.6% to 7.7% and 3.3% to 6.6% were found in response to hypercarbic normoxia and hypercarbic hyperoxia, respectively whereas CBF increased by 8.2% to 27.8% and 3.5% to 19.8% for hypercarbic normoxia and hypercarbic hyperoxia, respectively. Therefore, the change in BAT was generally observed to be smaller than the change in CBF and this effect was smaller for hypercarbic hyperoxia (used here) relative to hypercarbic normoxia. While these measurements were made in gray matter only, it is likely that a similar or smaller reduction in BAT persists in white matter. To reduce this potential confound, we used a pCASL approach that is known to be less sensitive to transit time changes than single post-labeling delay pulsed ASL approaches that do not account for bolus duration. This reduction in sensitivity is largest for tissue with shorter BAT values, such as healthy tissue. In regions where the BAT is much longer (e.g., white matter or ischemic tissue), it is possible that these changes could influence the CBF measurements. Given the relatively small change in BAT relative to CBF observed in our separate studies, and localization of most negative BOLD CVR regions to tissue that partial volumes primarily with gray matter (with the exception of patient 14), we do not anticipate that this is a major limitation of the current study. Nevertheless, these changes should be considered when interpreting the findings of this study. A related concern is that if the BAT changes with stimulation, the labeling efficiency of the pCASL measurement may also change. While we cannot rule out this effect, it is likely that the small change in BAT ($\sim$3.3% to 6.6% in gray matter) is mostly attributable to changes in flow velocity in smaller vessels experiencing changes in CBV, rather than in the large feeding cervical vessels where the blood–water labeling occurs. However, separate measurements of BAT changes in patients may be warranted and could help clarify the findings in voxels that contain substantial white matter contributions. It cannot be ruled out that a small increase in blood–water velocity during the hypercarbic stimulus may lead to a reduction in labeling efficiency, which would then lead to an underestimation in CBF if left unaccounted for in the model.

Partial volume contributions generally are also an inherent concern in ASL studies at typical spatial resolutions, as CBF in gray and white matter differs by approximately a factor of 2 to 3.[18] We have recently demonstrated how ASL-measured CBF values change with versus without partial volume corrections.[17,39] As expected, cortical CBF and BAT will increase and decrease, respectively, when correction routines are implemented for partial volume effects. Although such routines generally are most robust when ASL data are acquired with multiple postlabeling delay times, only a single delay was used here because of time considerations for the hypercarbic stimulus in patients. To reduce this confounding effect, we analyzed exactly the same regions in BOLD and ASL data, and therefore, partial volume contributions were identical between scans. Care was taken to ensure that absolute CBF numbers were not over interpreted; rather, the primary experimental measure was the change in the CBF-weighted signal between normocarbia and hypercarbia. We considered applying strict signal-to-noise ratio thresholds to this component of the study, but this was avoided as baseline CBF may be quite low in hypoperfused tissue and may significantly increase (or decrease) upon stimulation. We thus focused on statistically significant changes in ASL signal. However, owing to the above complications, absolute CBF values should be interpreted with caution.

We utilized a pairwise subtraction approach to calculate the CBF maps. It should be noted that more complex subtraction approaches have been proposed for ASL data, including surround and sinc subtraction.[40] A key feature of these elegant procedures is that they may reduce signal variability and improve sensitivity for detection of activated voxels in ASL data. Much of this improvement derives from transient changes in blood oxygenation and signal drift between control and label acquisitions that are reduced, and therefore, these methods are particularly important in experiments with short stimulus durations and/or when ASL maps themselves are being used for identification of activated voxels. Here, all data were corrected for baseline drift, our stimulus block durations were long (e.g., 3 minutes), and data were not analyzed until signal reached steady state within a stimulus or baseline block. Therefore, we chose to use a more basic subtraction approach. However, future studies would likely benefit from these more complex methods, especially those that use shorter stimulus durations or use ASL data to identify activated voxels (rather than BOLD data as was used here).

Finally, ASL scans were always performed after the BOLD scans, and $\sim$6 to 7 minutes of room air breathing occurred between the final BOLD hypercarbic block and first ASL hypercarbic block. While we anticipate this is sufficient time to allow blood gases, arterial oxygen saturations, and $EtCO_2$ values to return to baseline, vascular adaptation between scans cannot be ruled out as a possible complication in our study.

In summary, only a small fraction (3/15) of participants exhibiting negative BOLD reactivity to hypercarbic hyperoxic stimuli also had colocalizing reductions in CBF consistent with vascular steal. Therefore, additional mechanisms such as autoregulation and metabolism upregulation should be considered when interpreting negative BOLD reactivity.

DISCLOSURE/CONFLICT OF INTEREST

The authors declare no conflict of interest.

REFERENCES

1 Famakin BM, Chimowitz MI, Lynn MJ, Stern BJ, George MG. Causes and severity of ischemic stroke in patients with symptomatic intracranial arterial stenosis. *Stroke* 2009; **40**: 1999–2003.
2 Derdeyn CP, Chimowitz MI, Lynn MJ, Fiorella D, Turan TN, Janis LS *et al.* Aggressive medical treatment with or without stenting in high-risk patients with intracranial artery stenosis (SAMMPRIS): the final results of a randomised trial. *Lancet* 2014; **383**: 333–341.
3 Markus H, Cullinane M. Severely impaired cerebrovascular reactivity predicts stroke and TIA risk in patients with carotid artery stenosis and occlusion. *Brain* 2001; **124**(Pt 3): 457–467.
4 Zaca D, Hua J, Pillai JJ. Cerebrovascular reactivity mapping for brain tumor presurgical planning. *World J Clin Oncol* 2011; **2**: 289–298.
5 Gao YZ, Zhang JJ, Liu H, Wu GY, Xiong L, Shu M. Regional cerebral blood flow and cerebrovascular reactivity in Alzheimer's disease and vascular dementia assessed by arterial spinlabeling magnetic resonance imaging. *Curr Neurovasc Res* 2013; **10**: 49–53.
6 Wise RG, Harris AD, Stone AJ, Murphy K. Measurement of OEF and absolute CMRO: MRI-based methods using interleaved and combined hypercapnia and hyperoxia. *Neuroimage* 2013; **83C**: 135–147.
7 Zappe AC, Uludag K, Oeltermann A, Ugurbil K, Logothetis NK. The influence of moderate hypercapnia on neural activity in the anesthetized nonhuman primate. *Cereb Cortex* 2008; **18**: 2666–2673.
8 Fierstra J, Conklin J, Krings T, Slessarev M, Han JS, Fisher JA *et al.* Impaired peri-nidal cerebrovascular reserve in seizure patients with brain arteriovenous malformations. *Brain* 2011; **134**(Pt 1): 100–109.
9 Taylor CL, Selman WR, Ratcheson RA. Steal affecting the central nervous system. *Neurosurgery* 2002; **50**: 679–688, discussion 688-689.
10 Heyn C, Poublanc J, Crawley A, Mandell D, Han JS, Tymianski M *et al.* Quantification of cerebrovascular reactivity by blood oxygen level-dependent MR imaging and correlation with conventional angiography in patients with Moyamoya disease. *AJNR Am J Neuroradiol* 2010; **31**: 862–867.
11 Waltz AG. Effect of Pa CO2 on blood flow and microvasculature of ischemic and nonischemic cerebral cortex. *Stroke* 1970; **1**: 27–37.
12 Yamaguchi T, Regli F, Waltz AG. Effect of PaCO2 on hyperemia and ischemia in experimental cerebral infarction. *Stroke* 1971; **2**: 139–147.
13 Fieschi C, Agnoli A, Battistini N, Bozzao L, Prencipe M. Derangement of regional cerebral blood flow and of its regulatory mechanisms in acute cerebrovascular lesions. *Neurology* 1968; **18**: 1166–1179.
14 Rapela CE, Green HD. Autoregulation of canine cerebral blood flow. *Circ Res* 1964; **15: SUPPL**: 205–212.
15 Buxton RB, Wong EC, Frank LR. Dynamics of blood flow and oxygenation changes during brain activation: the balloon model. *Magn Reson Med* 1998; **39**: 855–864.
16 Sotero RC, Trujillo-Barreto NJ. Modelling the role of excitatory and inhibitory neuronal activity in the generation of the BOLD signal. *Neuroimage* 2007; **35**: 149–165.
17 Donahue MJ, Faraco CC, Strother MK, Chappell MA, Rane S, Dethrage LM *et al.* Bolus arrival time and cerebral blood flow responses to hypercarbia. *J Cereb Blood Flow Metab* 2014; **34**: 1243–1252.
18 van Osch MJ, Teeuwisse WM, van Walderveen MA, Hendrikse J, Kies DA, van Buchem MA. Can arterial spin labeling detect white matter perfusion signal? *Magn Reson Med* 2009; **62**: 165–173.
19 Gevers S, van Osch MJ, Bokkers RP, Kies DA, Teeuwisse WM, Majoie CB *et al.* Intra- and multicenter reproducibility of pulsed, continuous and pseudo-continuous arterial spin labeling methods for measuring cerebral perfusion. *J Cereb Blood Flow Metab* 2011; **31**: 1706–1715.
20 Wu WC, Fernandez-Seara M, Detre JA, Wehrli FW, Wang J. A theoretical and experimental investigation of the tagging efficiency of pseudocontinuous arterial spin labeling. *Magn Reson Med* 2007; **58**: 1020–1027.
21 Ashkanian M, Gjedde A, Mouridsen K, Vafaee M, Hansen KV, Ostergaard L *et al.* Carbogen inhalation increases oxygen transport to hypoperfused brain tissue in patients with occlusive carotid artery disease: increased oxygen transport to hypoperfused brain. *Brain Res* 2009; **1304**: 90–95.
22 Suzuki J, Takaku A. Cerebrovascular 'moyamoya' disease. Disease showing abnormal net-like vessels in base of brain. *Arch Neurol* 1969; **20**: 288–299.
23 Mugikura S, Takahashi S, Higano S, Shirane R, Sakurai Y, Yamada S. Predominant involvement of ipsilateral anterior and posterior circulations in moyamoya disease. *Stroke* 2002; **33**: 1497–1500.
24 Samuels OB, Joseph GJ, Lynn MJ, Smith HA, Chimowitz MI. A standardized method for measuring intracranial arterial stenosis. *AJNR Am J Neuroradiol* 2000; **21**: 643–646.
25 Jenkinson M, Smith S. A global optimisation method for robust affine registration of brain images. *Med Image Anal* 2001; **5**: 143–156.
26 Lu H, Clingman C, Golay X, van Zijl PC. Determining the longitudinal relaxation time (T1) of blood at 3.0 Tesla. *Magn Reson Med* 2004; **52**: 679–682.
27 Hare HV, Germuska M, Kelly ME, Bulte DP. Comparison of CO in air versus carbogen for the measurement of cerebrovascular reactivity with magnetic resonance imaging. *J Cereb Blood Flow Metab* 2013; **33**: 1799–1805.
28 Paulson OB. Regional cerebral blood flow in apoplexy due to occlusion of the middle cerebral artery. *Neurology* 1970; **20**: 63–77.
29 Donahue MJ, van Laar PJ, van Zijl PC, Stevens RD, Hendrikse J. Vascular space occupancy (VASO) cerebral blood volume-weighted MRI identifies hemodynamic impairment in patients with carotid artery disease. *J Magn Reson Imaging* 2009; **29**: 718–724.
30 Derdeyn CP, Videen TO, Yundt KD, Fritsch SM, Carpenter DA, Grubb RL *et al.* Variability of cerebral blood volume and oxygen extraction: stages of cerebral haemodynamic impairment revisited. *Brain* 2002; **125**(Pt 3): 595–607.
31 Thomas BP, Liu P, Aslan S, King KS, van Osch MJ, Lu H. Physiologic underpinnings of negative BOLD cerebrovascular reactivity in brain ventricles. *Neuroimage* 2013; **83C**: 505–512.
32 Scouten A, Constable RT. VASO-based calculations of CBV change: accounting for the dynamic CSF volume. *Magn Reson Med* 2008; **59**: 308–315.
33 Donahue MJ, Lu H, Jones CK, Edden RA, Pekar JJ, van Zijl PC. Theoretical and experimental investigation of the VASO contrast mechanism. *Magn Reson Med* 2006; **56**: 1261–1273.
34 Siero JC, Ramsey NF, Hoogduin H, Klomp DW, Luijten PR, Petridou N. BOLD specificity and dynamics evaluated in humans at 7 T: comparing gradient-echo and spin-echo hemodynamic responses. *PLoS One* 2013; **8**: e54560.
35 Donahue MJ, Ayad M, Moore R, van Osch M, Singer R, Clemmons P *et al.* Relationships between hypercarbic reactivity, cerebral blood flow, and arterial circulation times in patients with moyamoya disease. *J Magn Reson Imaging* 2013; **38**: 1129–1139.
36 Ashkanian M, Borghammer P, Gjedde A, Ostergaard L, Vafaee M. Improvement of brain tissue oxygenation by inhalation of carbogen. *Neuroscience* 2008; **156**: 932–938.
37 Donahue MJ, Strother MK, Hendrikse J. Novel MRI approaches for assessing cerebral hemodynamics in ischemic cerebrovascular disease. *Stroke* 2012; **43**: 903–915.
38 Petersen ET, Mouridsen K, Golay X. The QUASAR reproducibility study, Part II: results from a multi-center Arterial Spin Labeling test-retest study. *Neuroimage* 2010; **49**: 104–113.
39 Chappell MA, Groves AR, MacIntosh BJ, Donahue MJ, Jezzard P, Woolrich MW. Partial volume correction of multiple inversion time arterial spin labeling MRI data. *Magn Reson Med* 2011; **65**: 1173–1183.
40 Mumford JA, Hernandez-Garcia L, Lee GR, Nichols TE. Estimation efficiency and statistical power in arterial spin labeling fMRI. *Neuroimage* 2006; **33**: 103–114.

Supplementary Information accompanies the paper on the Journal of Cerebral Blood Flow & Metabolism website (http://www.nature.com/jcbfm)